Strojniški vestnik - Journal of Mechanical Engineering 60(2014)6, 375-381
DOI:10.5545/sv-jme.2013.1506
Original Scientific Paper
Received for review: 2013-10-14
Received revised form: 2014-02-10
Accepted for publication: 2014-02-28


# Influence of Plying Strategies and Trigger Type on Crashworthiness Properties of Carbon Fiber Laminates Cured through Autoclave Processing

Enrico Troiani* – Lorenzo Donati – Gianluca Molinari – Raffaella Di Sante
University of Bologna, MasterLab, Italy

*A small-scale experimental test able to characterize the energy absorption of a material under compression was developed by innovatively introducing self-supporting sinusoidal shape specimens, thus avoiding the complex anti-buckling devices of classical flat specimen tests. Two carbon-fiber-reinforced polymer (CFRP) pre-preg types were tested: 12 plies of unidirectional tape or 8 plies of plain weave fabric for a laminate approximately 1.8 mm thick in both cases. Three stacking sequences were analysed, in order to identify the configuration able to maximize the specific energy absorption (SEA), i.e. the energy absorbed per unit mass of crushed structure is expressed in J/g, with the unidirectional specimen providing the best results.*

*In order to have a controlled crush, the specimens were produced with different auto-triggering configurations. Indeed, the fibers' continuity was interrupted in selected position and to different degrees in order to investigate the SEA of the weakened laminates. For unidirectional specimens, the SEA maximum value and behaviour over the stroke were unaffected by the trigger position. Therefore, the auto-triggering configuration was able to control the position of the initial failure of the specimen without any decrease in safety performance.*
**Keywords: composites, compression test, crashworthiness, specific energy absorption (SEA)**

## 0 INTRODUCTION

The overall objective of designing for crashworthiness is to use the energy-absorption characteristics of structures in order to reduce injuries and fatalities in mild impacts, which are mostly due to the accelerations and load histories experienced by passengers. The energy-absorption effect can be attained either by modifying the structural geometry of the assembly or by introducing specific load-limiting devices into the structure, e.g. the controlled collapse of a vehicle ensures a safe dissipation of a given amount of kinetic energy.

Therefore, an important aspect of crashworthiness is the progressive failure of the structure, which is a controlled and predictable failure that progresses through the body at the loading speed. The progressive failure mechanism allows a larger amount of energy to be absorbed, compared to a catastrophic failure. The typical behaviour of a progressive failure in a crushed structure is shown in Fig. 1. The key parameters are the energy absorption (EA), which is the total energy absorbed and is represented by the area below the load-deformation curve, and the specific energy absorption (SEA), the energy absorbed per unit mass of the crushed sample.

Traditionally, in the particular case of aircraft, the energy-absorption devices are steel or aluminum structural elements; these materials allow a controlled collapse of the structure during which they absorb energy by folding or hinging, involving extensive plastic deformation. The current trend of substituting metals with composites, mostly carbon fibers-epoxy resins, can improve the energy absorption performance of the devices [2] and [3], but it introduces several problems due to the complexity of failure mechanisms that can occur within the material [4] to [7].

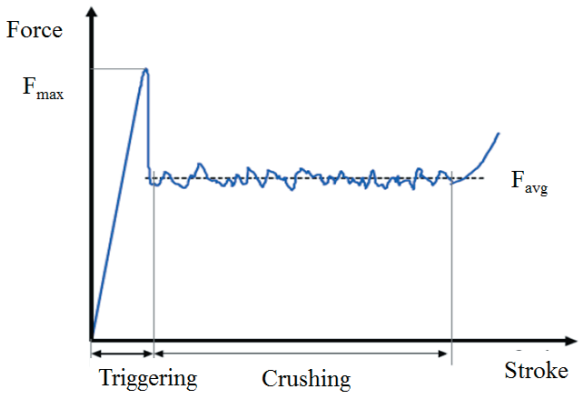


**Fig. 1.** *Typical force-stroke history [1]*

Moreover, many studies indicate that the energy absorption characteristics in composite structures are strictly dependant on the crushing triggers [8] to [10], i.e. weakened areas at appropriate locations [11] and [12], which are useful in initiating a stable and controlled progressive failure. Bevels and chamfers are very effective in the preventing catastrophic failures [13], thus providing a stable propagation of the collapse, while at the same time reducing the peak load at the initial failure. More advanced and effective

*Corr. Author's Address: University of Bologna, MasterLab, via Fontanelle 40, 47121 Forlì, Italy, enrico.troiani@unibo.it

technical solutions using shape memory alloys [14] have been introduced, at the expense of a more complex manufacturing.

However, there is a lack of information about the behaviour of these structures under operative loads, because the introduction of composite materials makes the data obtained from the incidents and accidents of existing metallic aircrafts no longer representative. The behaviour of composite structures can be described through extensive substructure testing within a building block approach to the design of crashworthy structures. Numerical models of both structural and material behaviour, supported by tests of coupons or small structures, are the preferred choice for understanding the behaviour of these structures

In the literature, the available coupon size test methods for the energy absorption determination of composite materials can be divided into two main categories based on the kind of specimen used: flat specimen and self-supporting specimen, usually thin walled tubes. The flat specimen test method, which is easier and less expensive, consists of crushing a rectangular specimen constrained in a dedicated anti-buckling fixture [15] and [16]. However, the overall procedure is influenced by many external parameters like the complex fixture or the test operator's skills.

The self-supporting specimen test method eliminates the need for an anti-buckling fixture and all its related issues, like the phenomenon of fronds tearing or the arbitrary closing force of the specimen. The different shapes for the self-supporting specimens found in the literature range from a simple tube, round or square, to sinusoidal webs [17] to complex C-shaped tube-segments like the ones developed by DLR [18]. The manufacture of tubes is more complex than that of flat specimens, requiring an internal mandrel around which the plies have to be wrapped.

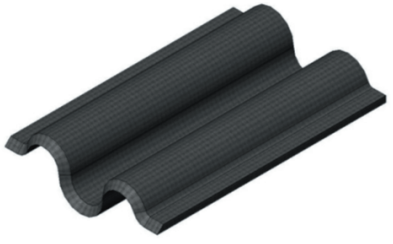

**Fig. 2.** *Example of self-supporting specimen, 3HC shape*

In order to define a simple and useful tool for the design of crashworthiness in composite materials, an innovative test method for the energy absorption determination has been developed [19] to [21]. The study led to a new concept for a corrugated specimen, as shown in Fig. 2, which is easier to produce than the ones proposed in the literature.

The main goal of this research has been therefore the better understanding of SEA behaviour in a corrugated specimen, together with optimization of the crush initiator.

Crush tests of two pre-preg systems were performed to evaluate the SEA behaviour. After observation of the failure modes, a new trigger geometry was tested in the same materials.

## 1 EXPERIMENTAL PROCEDURE

The specimens' material is a carbon fiber reinforced epoxy matrix. Two pre-preg systems were tested: 12 plies of unidirectional (UD) tape (ACG T700 24k/MTM57) or 8 plies of plain weave (PW) fabric (GG200P/IMP530R), for the production of a laminate of around 1.8 mm thickness in both cases. Both materials were cured in an autoclave, according to the supplier indications at 120 °C for 1 h for unidirectional tape and 0.5 h at 120 °C then 0.5 h at 150 °C for plain weave, both under 6.2 bar compacting pressure. Three stacking sequence (UD $[0/90]_{3s}$, PW0/90° and PW±45°) were tested in order to identify the configuration able to maximize the SEA.

Once machined, each plate is about 210×180 mm and 1.8 mm thick. Six specimens per plate can be cut, four with three repetitions of the half-circular modulus (60×80 mm, called 3HC) and two with five repetitions (80×, called 5HC).

At first, all the specimens were triggered with a simple 45° single side chamfer trigger, as shown in Fig. 3, due to its ease of use.

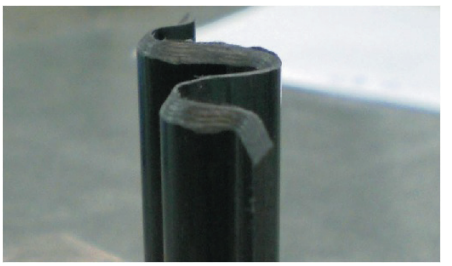

**Fig. 3.** *Trigger chamfer configuration*

Each specimen was tested in a vertical configuration, as shown in Fig. 4, compressed between two steel plates that slide along four steel shafts with self-aligning ball bearings at a quasi-static speed rate of 50 mm/min. A displacement of half the height of the specimen is imposed. Performing the tests at a quasi-static rate does not influence the test results: even if there is a lack of consensus about the

influence of test speed on the energy absorption in the literature, a side test campaign confirmed that it does not affect the SEA [21]. The load and displacements were recorded.

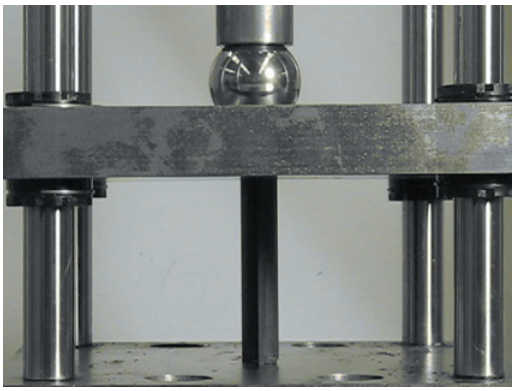

**Fig. 4.** *Testing configuration*

## 2 RESULTS AND DISCUSSION

From the SEA point of view, the chamfer trigger works perfectly, initiating the crushing smoothly up to an almost steady level of sustained load, as shown in Fig. 5, where the SEA stroke behaviour for the tested specimens is reported.

The EA can be calculated as the total area under the force-stroke diagram. The SEA is the energy absorbed per unit mass, where stroke l, cross-sectional area A, and density $\rho$ [21] thus:

$$SEA = EA / (\rho A l) . \quad (1)$$

As might be expected, the maximum energy is absorbed by the UD [0/90]3s specimens due to the material having better mechanical properties, thus providing a maximum value of 100 J/g for SEA, which was stable all along the compression stroke. The UD specimen collapse is mostly due to a mechanism combining lamina bending and fragmentation.

A chamfer trigger is therefore an excellent solution for the experimental tests, as it is both simple and quick to execute. However, as an effective practical application (for example, as energy absorbers situated behind the bumper of a vehicle), a small drawback consists in the difficulty of adequately supporting and fixing the chamfered end of the component. More generally, post curing mechanical machining constitutes an additional operation, which is not negligible in terms of time and resources in the production phase of the test, and which can generate local defects and micro-cracks, that, in turn, influence the test results.

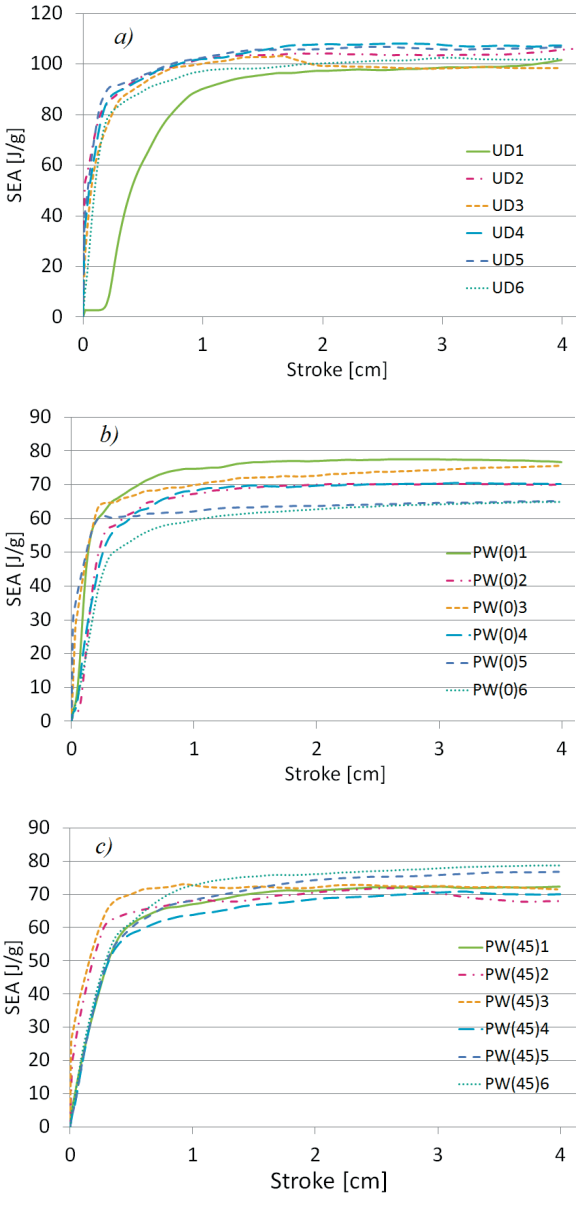


**Fig. 5.** *SEA Stroke behaviour; a) UD, b) PW 0/90° and c) PW ±45°*

A very promising way to solve the aforementioned problems of the chamfer trigger consists in creating a localized weakening of the specimen directly in the lamination phase. One of the simplest solutions is to insert in the stacking sequence some shorter layers, in order to obtain a specimen which presents a reduced number of layers at one end (called an ATF configuration), as shown in Fig. 6. This is a pre-curing process with no supporting problems in the test phase.

A testing campaign on this auto-trigger configuration was carried out on the same [0/90]3s stacking sequence of UD tape (ACG T700 24k/ MTM57). The SEA-stroke behaviour is shown in

Fig. 7. The achieved levels of SEA are close to those obtained with the 45° single side chamfer trigger.

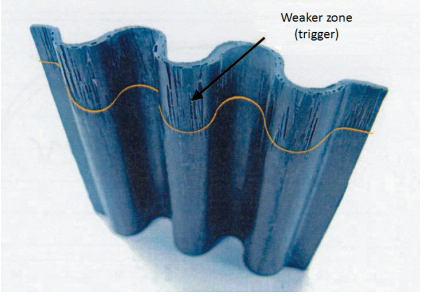


**Fig. 6.** *ATF-trigger specimen*

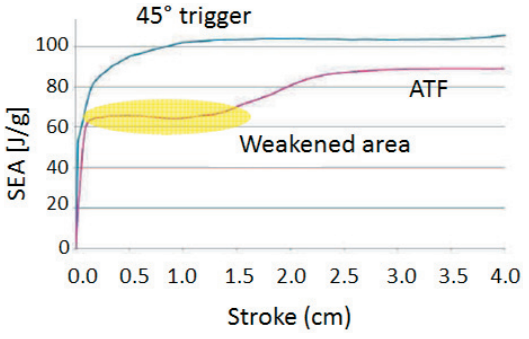


**Fig. 7.** *SEA comparison between UD 45° chamfer and UD ATF trigger specimen*

Unfortunately, the SEA trend is not optimal: the SEA value begins to climb (rather slowly) to significant levels only after rupture of the entire trigger. This is due to the large weakening area, which prevents a rapid rise in specific energy. Furthermore, there is a substantial lack of resin in the trigger area, as shown in Fig. 6, thereby generating lower and non-uniform mechanical properties.

In order to overcome the drawbacks of the ATF configuration, avoiding the lack of fibers in specific areas and getting a trigger that is as small as possible (in order to maximize the SEA), a new type of trigger configuration has been conceived: on each weakened lamina, a strip is cut (as in the ATF configuration) but not discarded, and is therefore laminated in the mold together with the remaining part of the sheet. Fig. 8 shows an example of the standard and weakened laminae with the new auto-trigger for the 0 and 90° layers. If the cut is on the 90° laminae, the weakening is achieved through a reduction of fiber content in the zone (resin properties dominated zone), while when the weakening is realized on the 0° laminae, a discontinuity in the fibers is deliberately introduced. In a similar way the configurations PW 45* and PW 0/90* were realized.

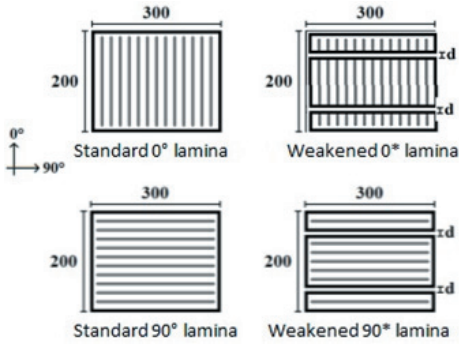


**Fig. 8.** *New trigger configuration*

This simple solution avoids the problem of a lack of resin on the trigger because the small thickness "d" of the gap is easily filled by an excess of resin in the prepreg. Moreover, unlike the ATF configuration, this new idea involves the use of a very narrow trigger (only 5 mm strips compared with 20 mm of the ATF), in order to increase the level of SEA.

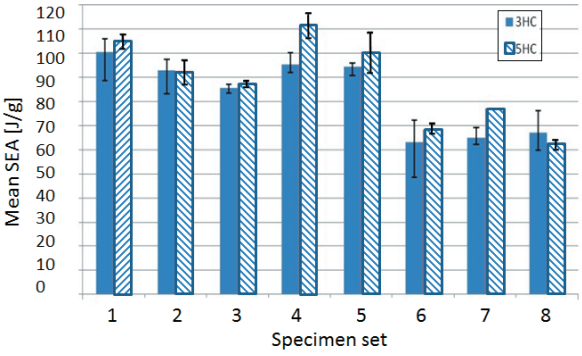


**Fig. 9.** *Comparison of SEA values for 3HC and 5HC specimens*

A new test campaign on this auto-trigger configuration was carried out on the same materials and stacking sequences of previous UD and PW specimens. The stacking sequences are reported in detail in Table 1, where the symbol * is used to identify the weakened laminae. The measured values of loads and SEA are not dependent on the number of semi-circular repetitions: the 3HC and 5HC specimen results are comparable, as shown in Fig. 9 for the SEA.

As can be seen from Table 1, Set 1 has four weakened layers in the inner 90° laminae where d = 0 mm, i.e. without any interrupted fiber. Moreover, during the curing process the matrix becomes partially fluid and fills the voids, recreating the material continuity. As a result, these specimens are considered not to be triggered, and can also be a benchmark for comparison with data from Fig. 5a. Their SEA behaviour is shown in Fig. 10.

**Table 1.** *New trigger configurations stacking sequences*

| Set no. | Features | layup |
|---|---|---|
| 1 | UD [0 ; 90*]3s; d = 0 mm | 0 – 90 – 0 – 90* – 0 – 90* – 90* – 0 – 90* – 0 – 90 – 0 |
| 2 | UD [0 ; 90*]3s; d = 2 mm | 0 – 90 – 0 – 90* – 0 – 90* – 90* – 0 – 90* – 0 – 90 – 0 |
| 3 | UD [0* ; 90]3s; d = 0 mm | 0 – 90 – 0* – 90 – 0* – 90 – 90 – 0* – 90 – 0* – 90 – 0 |
| 4 | UD [0* ; 90]3s; d = 0 mm | 0 – 90 – 0 – 90 – 0* – 90 – 90 – 0* – 90 – 0 – 90 – 0 |
| 5 | UD [0 ; 90*]3s; d = 2 mm | 0 – 90 – 0 – 90 – 0* – 90 – 90 – 0* – 90 – 0 – 90 – 0 |
| 6 | PW [0/90; 45*]2s; d = 0 mm | 0/90 – 45* – 0/90 – 45 – 45 – 0/90 – 45* – 0/90 |
| 7 | PW [0/90]4s; d = 0 mm | 0/90 – 0/90* – 0/90 – 0/90 – 0/90 – 0/90 – 0/90* – 0/90 |
| 8 | PW [0/90]4s; d = 0 mm | 0/90 – 0/90 – 0/90 – 0/90* – 0/90* – 0/90 – 0/90 – 0/90 |

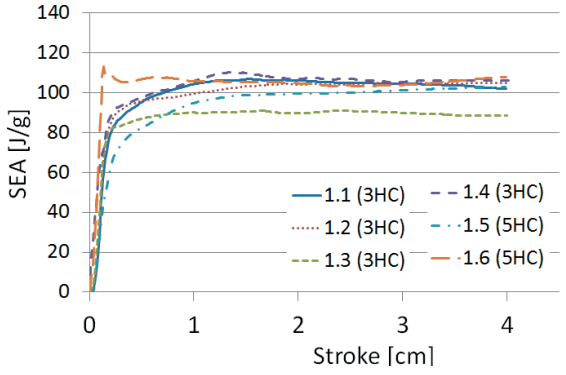


**Fig. 10.** *SEA behaviour in Set 1 - 6 specimens*

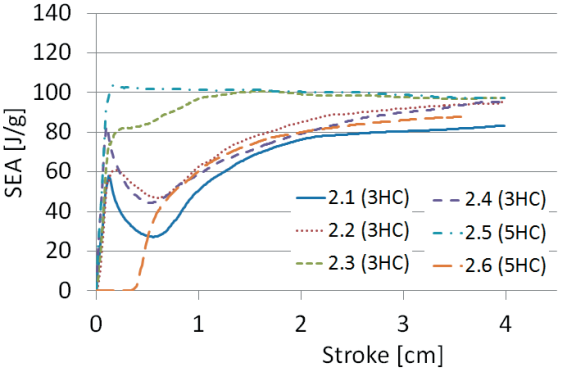


**Fig. 11.** SEA behaviour in Set 2 - 6 specimens

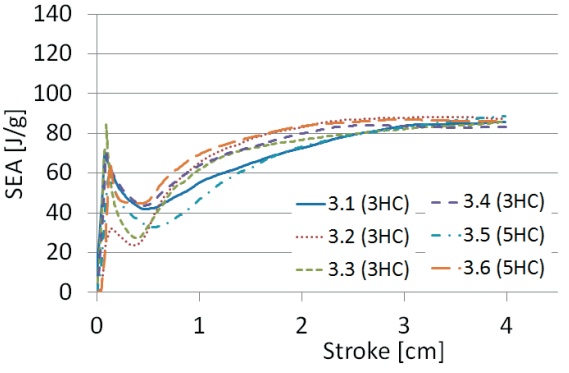


**Fig. 12.** *SEA behaviour in Set 3 - 6 specimens*

Analyzing the test results of Sets 1 and 2 (Fig. 11), it is noticeable that increasing the d values from 0 to 2 mm (on four layers) makes the specimens more sensitive to the presence of the trigger, as shown by the decrease in SEA values immediately after the initial peak. This transient phenomenon in the SEA-stroke behaviour is mostly due to the wide strip of resin, which results in too weak a trigger. A 10% lower average SEA and higher dispersion of results are related to the higher sensitivity to the trigger.

Conversely, cutting the 0° fibers brings about a greater degree of weakening: the fibers, in fact, are irreversibly broken in relation to the trigger, and the empty spaces are again filled by the resin with lower mechanical properties. As a consequence, the Set 3 results in Fig. 12 show high SEA peaks and immediate collapse loads. In these specimens, four of the 0°-layers were weakened, thus generating the drastic reduction in SEA performance.

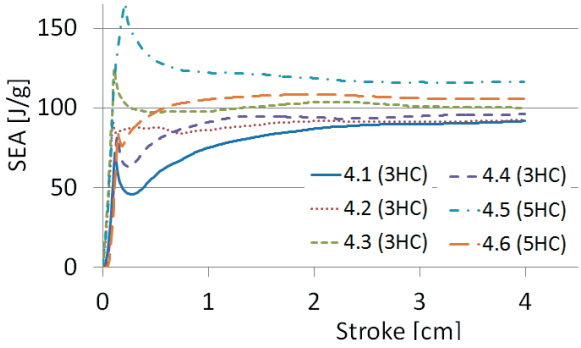


**Fig. 13.** *SEA behaviour in Set 4 - 6 specimens*

By reducing the number of split layers (Set 4, Fig. 13), the magnitude of the weakening is clearly lower than in Set 3, which reduces the sensitivity to the trigger and decreases the SEA. Thanks to the high values of SEA and the very short transition, Set 4 is an optimum configuration from the point of view of the absorption energy, although there is still an excessive variability in behaviour in the initial transient.

Similarly, in Set 5, where d is increased to 2 mm and it is more difficult to fill in the voids in the matrix, the values of SEA (Fig. 14) are fairly stable

and, on average, comparable to Set 4. As seen in the previous set, very high SEA values were found and were comparable to the reference condition (Set 1), on average about 100 J/g, after a very short transient.

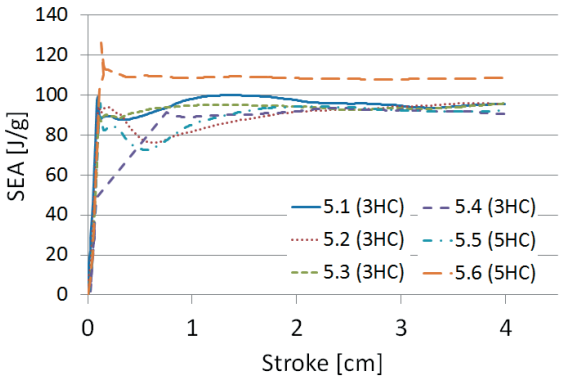


**Fig. 14.** *SEA behaviour in Set 5 - 6 specimens*

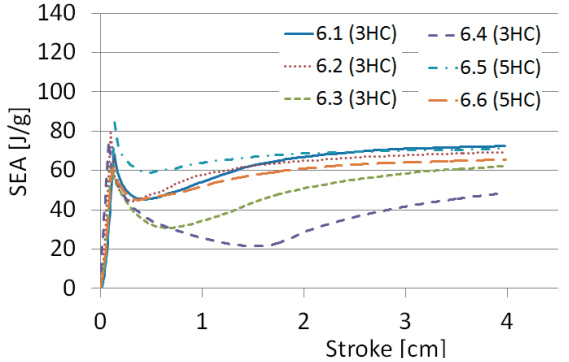


**Fig. 15.** *SEA behaviour in PW specimens (set n.6)*

The performance of PW specimens is obviously worse than the UD, due to the lower mechanical properties of the material. Another interesting difference is a noticeable "softening" of the SEA curves, as shown in Fig. 15. The range of stroke required to reach the equilibrium is much larger than in previous sets, which indicates an unstable crush and the presence of local unpredictable phenomena.

Another important issue is the failure mode of the specimens: the UD prepreg failures are due to the mixed contribution of transverse shearing and plate bending. For the PW fabric specimens, the intertwining of fibers at 0 and 90° interferes with the respective free deformation, thus generating a very large number of breaks extremely close together. This effect produces a very large number of tiny shards, which accumulate as debris at the base of the specimen. This kind of failure is considerably more stable and therefore very favorable for crashworthiness applications. However, the limited mechanical properties of PW fabric significantly reduced the absorption capacity. Fig. 16 shows typical broken specimens for both UD and PW configurations.

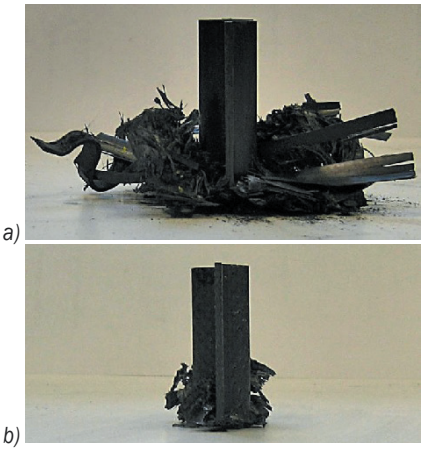


**Fig. 16.** *Failure modes; a) UD, and b) PW*

A direct comparison between the UD and PW specimen SEA behaviour is shown in Fig. 17. The behaviour of UD Set 2 specimens, a sharp peak followed by a drop, shows a different initial transient when compared to the reference set, although there is a similar mean value of SEA (differences less than 10%). Conversely, the weaker mechanical properties of the PW greatly reduce the energy absorption, with a collapse at very low levels (20 J/g) and SEA mean values more than 30% lower than those of UD.

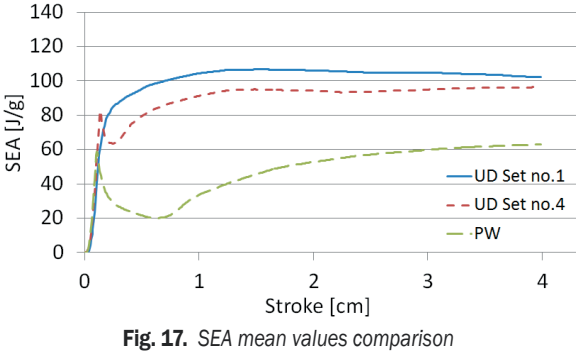


**Fig. 17.** *SEA mean values comparison*

## 3 CONCLUSIONS

The main achievement of the present paper is the definition of a reliable and affordable experimental procedure for the quantification of the energy absorption capability of composite materials. This work also constitutes the first step of a building block approach program that, starting from experimental tests on small specimens and numerical analysis, helps the designer to build up knowledge to better focus the study of more complex structures.

The results obtained from the experimental campaign showed that the test method using self-supporting specimens is reliable and, most important, is not affected by external factors introduced by the anti-buckling fixture, which is necessary in the flat specimens test procedure. Moreover, the sine wave specimens are easier to manufacture than the widely used tubes.

Regarding the other important feature for a crashworthy structure, namely the ability to control the position of the initial damage and its propagation, the auto-triggering configurations, with fiber continuity interrupted in selected positions and to various extents, proved to be a viable alternative to external triggers. The achieved levels of SEA for Sets 1, 4 and 5 are close to those obtained with the traditional chamfer configuration in UD, while eliminating time-consuming, post-curing, mechanical machining.

## 4 REFERENCES


[1] VV.AA. (2012). Chapter 14 – Crashworthiness and Energy Management. *Composite Materials Handbook CMH-17-3G, vol. 3.* SAE International, Washington D.C. USA, p. 1-9.

[2] Jacob, G.C., Fellers, J.F., Simunovic, S., Starbuck, J.M. (2002). Energy absorption in polymer composites for automotive crashworthiness. *Journal of Composite Materials*, vol. 36, no. 7, p. 813-850, DOI:10.1177/0021998302036007164.

[3] Carruthers, J.J., Kettle, A.P., Robinson, A.M. (1998). Energy absorption capability and crashworthiness of a composite material - a review. *Applied Mechanics Review*, vol. 51, no. 10, p. 635-649, DOI:10.1115/1.3100758.

[4] Hull, D. (1991). A unified approach to progressive crushing of fibre-reinforced composite tubes. *Composites Science and Technology*, vol. 40, no 4, p. 377-421, DOI:10.1016/0266-3538(91)90031-J.

[5] Farley, G.L., Jones, R.M. (1992). Crushing characteristics of continuous fiber-reinforced composite tubes. *Journal of Composite Materials*, vol. 26, no. 1, p. 37-50, DOI:10.1177/002199839202600103.

[6] Mamalis, A.G., Robinson, M., Manolakos, D.E., Demosthenous, D.A., Ioannidis, M.B., Carruthers, J. (1997). Crashworthy capability of composite material structures. *Composite Structures*, vol. 37, no. 2, p. 109-134, DOI:10.1016/S0263-8223(97)80005-0.

[7] Bolukbasi, A.O., Laananen, D.H. (1995). Analytical and experimental studies of crushing behavior in composite laminates. *Journal of Composite Materials*, vol. 29, no. 8, p. 1117-1139, DOI:10.1177/002199839502900806.

[8] Thornton, P.H. (1979). Energy absorption in composite structures. *Journal of Composite Materials*, vol. 13, no. 3, p. 247-262, DOI:10.1177/002199837901300308.

[9] Thornton, P.H. (1982). Energy absorption in composite tubes. *Journal of Composite Materials*, vol. 16, no. 6, p. 521-545, DOI:10.1177/002199838201600606.

[10] Farley, G.L. (1983). Energy absorption of composite materials. *Journal of Composite Materials*, vol. 17, p. 267-279, DOI:10.1177/002199838301700307.

[11] Sigalas, I., Kumosa, M., Hull, D. (1991). Trigger mechanisms in energy-absorbing glass cloth/epoxy tubes. *Composites Science and Technology*, vol. 40, no. 3, p. 265-287, DOI:10.1016/0266-3538(91)90085-4.

[12] Thuis, H.G.S.J., Metz, V.H. (1994). The influence of trigger configuration and laminate lay-up on the failure mode of composite crush cylinders. *Composite Structures*, vol. 28, no. 2, p. 131-137, DOI:10.1016/0263-8223(94)90043-4.

[13] Song, H.W., Du, X.W., Zhao, G.F. (2002). Energy absorption behavior of double-chamfer triggered glass/epoxy circular tubes. *Journal of Composite Materials*, vol. 36, no. 18, p. 2183-2198, DOI:10.1177/0021998302036018515.

[14] Huang, J.C., Wang, X.W. (2010). Effect of the SMA trigger on the energy absorption characteristics of cfrp circular tubes. *Journal of Composite Materials*, vol. 44, no. 5, p. 639-651, DOI:10.1177/0021998309347572.

[15] Lavoie, J.A., Kellas, S. (1996). Dynamic crush tests of energy-absorbing laminated composite plates. *Composites: Part A Applied Science and Manufacturing*, vol. 27, no. 6, p. 467-475, DOI:10.1016/1359-835X(95)00058-A.

[16] Cauchi Savona, S., Hogg, P.J. (2005). Investigation of plate geometry on the crushing of at composite plates. *Composites Science and Technology*, vol. 66, no. 11-12, p. 1639-1650, DOI:10.1016/j.compscitech.2005.11.011.

[17] Farley, G.L., Jones, R.M. (1989). *Energy-absorption capability of composite tube and beams*. NASA Technical Publications TM 101634:1-248, Hampton.

[18] Kohlgruber, D., Kamoulakos, A. (1998). Validation of numerical simulation of composite helicopter subfloor structures under crush loading. *Proceedings of the 54th AHS Annual Forum*, Washington, D.C.

[19] Garattoni, F., Molinari, G., Troiani, E. (2010). Development of a reliable test to support and validate a numerical model of progressive damage for composite materials. *Proceedings of the Royal Aeronautical Society 2nd Aircraft Structural Design Conference*, London.

[20] Garattoni, F., Troiani, E. (2010). An experimental method and numerical simulation for composite materials energy absorption determination. *Proceedings of the 27th International Congress of the Aeronautical Sciences*. Nice.

[21] Feraboli, P. (2008). Development of a corrugated test specimen for composite materials energy absorption. *Journal of Composite Materials*, vol. 42, no. 3, p. 229-256., DOI:10.1177/0021998307086202.